



Original article

## Preparation and evaluation of antidiabetic activity of mangiferin-loaded solid lipid nanoparticles

Ahmed I. Foudah<sup>\*</sup>, Mohammad Ayman Salkini, Mohammed H. Alqarni, Aftab Alam<sup>\*</sup>

Department of Pharmacognosy, College of Pharmacy, Prince Sattam Bin Abdulaziz University, Alkharj 11942, Saudi Arabia



### ARTICLE INFO

#### Keywords:

Mangiferin  
Diabetes  
Prophylactic mechanisms  
Nanoparticles

### ABSTRACT

This study aimed to develop and optimize mangiferin-loaded solid lipid nanoparticles (MG-SLNs) using the microemulsion technique and ultrasonication. The MG-SLNs were composed of Labrafil M 2130 CS, MG, ethanol, Tween 80, and water. The optimized MG-SLNs exhibited a particle size of  $138.37 \pm 3.39$  nm, polydispersity index of  $0.247 \pm 0.023$ , entrapment efficiency of  $84.37 \pm 2.43$  %, and zeta potential of  $18.87 \pm 2.42$  mV. Drug release studies showed a two-fold increase in the release of MG from SLNs compared to the solution. Confocal images indicated deeper permeation of MG-SLNs, highlighting their potential. Molecular docking confirmed mangiferin's inhibitory activity against  $\alpha$ -amylase, consistent with previous findings. In vitro studies showed that MG-SLNs inhibited  $\alpha$ -amylase activity by  $55.43 \pm 6.11$  %,  $\alpha$ -glucosidase activity by  $68.76 \pm 3.14$  %, and exhibited promising antidiabetic activities. In a rat model, MG-SLNs significantly and sustainably reduced blood glucose levels for up to 12 h. Total cholesterol and triglycerides decreased, while high-density lipoprotein cholesterol increased. Both MG-SOL and MG-SLNs reduced SGOT and SGPT levels, with MG-SLNs showing a more significant reduction in SGOT compared to MG-SOL. Overall, the biochemical results indicated that both formulations improved diabetes-associated alterations. In conclusion, the study suggests that loading MG in SLNs using the newly developed approach could be an efficient oral treatment for diabetes, offering sustained blood glucose reduction and positive effects on lipid profiles and liver enzymes.

### 1. Introduction

The discovery of the sweet nature of urine by the ancient Greek, Indian and Egyptian civilizations led to the spread of the term "diabetes mellitus," a metabolic condition marked by abnormalities in insulin production, insulin action, or both causing persistent hyperglycemia and most frequently identified using either the estimate of plasma glucose (FPG or OGTT) or HbA1c (Sapra and Bhandari, 2021). Various subtypes were type 1, type 2, maturity-onset diabetes of the young, gestational diabetes, neonatal diabetes and steroid-induced diabetes (Chaudhury et al., 2017; Kharroubi, 2015). Diabetes patients are more likely to experience significant health issues such as myocardial infarction, stroke, renal failure, eyesight loss, and early death (Chaudhury et al., 2017). According to the 10th publication of the IDF Diabetes Atlas 2021, more than one in ten adults is diabetic, and this rate of growth is expected to continue. The global frequency of diabetes among grown-ups age between 20 and 80 in 2021 was 10.5 % (536.6 million), and it was expected to expand to 12.2 % (783.2 million) in 2045 (Sun et al., 2022).

Mangifera indica, a member of the Anacardiaceae family of plants and popularly recognized for its sweetness, is grown on over 3.7 million hectares of land worldwide (Samanta, 2022). Several different phytochemicals that were reported from M. indica. Out of these polyphenols—including mangiferin (MG), catechins, gallic acid, kaempferol, quercetin, protocatechuic acid, propyl and methyl gallate, ellagic acids, anthocyanins and rhamnetin are the most prevalent chemical types in M. indica (Ngo et al., 2019). These phenolic compounds have powerful antioxidant activity that is beneficial for defending human tissues against oxidative stress. They also have antidiabetic, anti-oxidant, anti-inflammatory, anti-lithiatic, and anti-carcinogenic characteristics (Samanta, 2022). The World Health Organization advises using natural medications to manage diabetes. Mango is one of those medicinal plants that are used successfully in several societies to cure diabetes (Sun et al., 2022).

<sup>\*</sup> Corresponding authors.

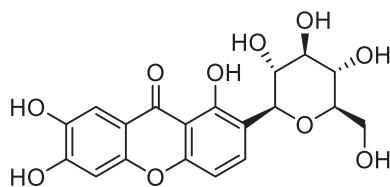
E-mail addresses: [a.foudah@psau.edu.sa](mailto:a.foudah@psau.edu.sa) (A.I. Foudah), [m.salkini@psau.edu.sa](mailto:m.salkini@psau.edu.sa) (M. Ayman Salkini), [m.alqarni@psau.edu.sa](mailto:m.alqarni@psau.edu.sa) (M.H. Alqarni), [a.alam@psau.edu.sa](mailto:a.alam@psau.edu.sa) (A. Alam).

<https://doi.org/10.1016/j.sjbs.2024.103946>

Received 12 December 2023; Received in revised form 24 January 2024; Accepted 2 February 2024

Available online 8 February 2024

1319-562X/© 2024 The Authors. Published by Elsevier B.V. on behalf of King Saud University. This is an open access article under the CC BY-NC-ND license (<http://creativecommons.org/licenses/by-nc-nd/4.0/>).



**Mangiferin**

Mangiferin is a biological material found in different sections of mango trees, especially in the leaves, bark, and fruit. The growing interest in current years is attributed to the potential health benefits of mangiferin (Miura et al., 2001; Ichiki et al., 1998). However, similar to many natural compounds, mangiferin poses formulation challenges. It exhibits limited water solubility, potentially restricting its bioavailability and efficacy (Liu et al., 2020; Santonocito et al., 2022). This solubility issue creates hurdles for developing aqueous-based formulations like oral solutions or suspensions. Mangiferin is prone to degradation when subjected to heat, light, and extreme pH conditions. Additionally, its restricted permeability across biological membranes, such as the intestinal epithelium, hampers absorption and bioavailability. The identified obstacles can potentially be addressed by incorporating mangiferin into Solid Lipid Nanoparticles (SLN) (Zhang et al., 2021). The loading of mangiferin in the SLN would result in preventing it from the acidic pH of the stomach thus, making it to reach the intestine.

In addition, the self-emulsifying excipients used in the formulation of SLN results in absorption through lipase-mediated chylomicron development into the lymphatic system which then upsurges the absorption in addition to microfold cell and paracellular uptake. After this the mangiferin can be efficiently transported to the blood flow by intestinal lymphatics via thoracic lymph duct through microfold cell absorption. Because lymphatic capillaries' intercellular connections are more permeable than blood capillaries at the capillary level, SLN then is molecularly sieved into the bloodstream lymphatics instead of the way to the blood capillaries (Zhang et al., 2021; Date et al., 2020). Due to which, the therapeutic efficacy is increased, thus augmenting the bioavailability and mean residence time of the mangiferin in the blood. However, lymphatic administration is useful for targeting drug carriers to the lymphatics as well as for the absorption of medications that are poorly soluble in the body. In addition, lymphatic distribution of SLN enhances the plasma concentration of mangiferin while avoiding the hepatic first-pass effect (Mukherjee et al., 2009). In addition, the mangiferin released in the blood from the formulation after getting absorbed in intestine would ultimately reach the organs where alpha ( $\alpha$ ) – amylase is being synthesized namely pancreas and salivary glands (Cirri et al., 2018). The released  $\alpha$ - amylase is inhibited in the blood by mangiferin and the inhibited enzyme is not available for the breakdown of starch in the intestinal lumen.

Docking studies are to predict and understand the interactions between a small molecule (ligand) and a biological macromolecule (usually a protein). The primary purpose of docking studies is to explore the potential binding modes of a ligand within the active site or binding pocket of the target protein. This study gives an insight into the drug mode of action which are later validated by *in-vitro* and *in-vivo* parameters. Although mangiferin has previously published to show its anti-diabetic properties by inhibiting alpha-amylase enzyme, a confirmatory study was done by randomly choosing some antidiabetic targets and docking them with mangiferin.

When related to other systems, SLNs have several advantages, such as simplicity of formation, high scale production, low cost, good release profile, excellent physical stability, preparation without the use of organic solvents, chemical versatility, no toxicity of the lipid carrier system, biodegradability of the lipids, being less expensive than polymeric carriers, being more reliable, and biodegradability of the lipids, which improves the performance of pharmaceuticals (Varshosaz et al.,

2010).

MG faces several challenges when given orally, mainly because of its limited solubility, reduced bioavailability, significant hepatic first-pass metabolism, and notable P-gp efflux. Addressing these issues, it's crucial to develop a delivery system for MG that can enhance its bioavailability and ultimately elevate its concentration in the bloodstream. Therefore, the current work meant to formulate MG-loaded SLNs to rise the oral bioavailability of the MG by enhancing the solubility of the MG in the desired lipid that would increase the permeation of MG across the intestine, thus improving the absorption of the MG that would help in modulating  $\alpha$ -amylase and display anti-diabetic potential. The developed formulation will surely help in achieving the sole purpose, i. e., to manage diabetes using phytoconstituents and be safer in comparison to synthetic drugs.

## 2. Material and methods

### 2.1. Materials

MG was procured from Sigma Aldrich, Mumbai. Solid lipids such as Glycerol monostearate, Stearic acid, Palmitic acid, Cetylpalmitate, Deconic acid, Glycerol palmitostearate, gelucire 44/14, Labrafil M 2130 CS and poloxamer 188 were procured from Gattefosè. Surfactants such as Tween 80, Solutol, Labrasol, Tween 60, Transcutol, and Tween 20 from Gattefosè. DPPH and Alpha-amylase were bought from Sigma-Aldrich. Acarbose and metformin were acquired from the dispensary shop in Delhi. All other chemicals were used are of analytical grade.

### 2.2. Animals

Male Wistar rats having weight of 250 gm used in various animal experiments. The examination involving animals was conducted in accordance with the guidelines set forth by the Standing Committee of Bioethics Research at Prince Sattam bin Abdulaziz University in Al-Kharj, Saudi Arabia. The committee approved the use of animals in the research project (SCBR-020–2023) after careful consideration of the ethical implications and potential benefits of the study.

### 2.3. Method

#### 2.3.1. Selection of solid lipid and surfactant

Various solid-lipids, namely glyceryl monostearate, palmitic acid, stearic acid, Cetylpalmitate, Deconic acid, glycerol palmitostearate, Gelucire 44/14, Labrafil M 2130 CS and poloxamer 188 were selected according to the solubility of MG in the respective solid lipid. Therefore, 1 g of solid lipid was taken in a vial and in which MG was added incrementally until the saturated solubility was achieved. The glass vial was placed on the magnetic stirrer at a temperature above the melting point. It was noted how much MG was getting dissolved in particular solid lipids. The production of a clean, transparent mixture served as proof of full disintegration (Naseri et al., 2015; Qamar et al., 2021). In the case of the selection of surfactant, lipophilicity was taken into consideration. For this, a glass vessel was filled with 150 ml of solvent and 1 g of MG. 10 ml of the solution was taken, and they underwent a 20-minute centrifugation process at 2200 rpm. A 0.45 m membrane was used to filter samples to remove powdered solid MG (Cometa et al., 2020; Li et al., 2009).

#### 2.3.2. Preparation of SLNs

The development of SLN was made by the microemulsion technique trailed by sonication, in which the oil phase and aqueous phase were made independently. The oily part was composed of Labrafil M 2130 CS, MG, and ethanol, whereas the aqueous phase consisted of Tween 80 and water. Both parts were kept at the similar temperature, i.e.,  $75 \pm 2$  °C, and stirred at 800 rpm for 35 mins. After this, the hydrophilic part was added to the lipid part, that later treated with the sonication for 150

sec. This step was followed by pouring emulsion into the cold water that was then diluted to a final concentration of 25 ml which was allowed to be agitated for 4 mins. This developed formulation was then passed through a homogenizer (Stansted Fluid Power Ltd. ESSEX, U.K.) at 7000 rpm (Duong et al., 2020).

### 2.3.3. Optimization of MG-loaded SLNs

SLNs were optimized by the Design Expert (ver. 12, State-Ease Inc Minneapolis, USA) software was used. One of the widely employed designs, i.e., CCRD, was used for formulation optimization (Hassan et al., 2021). The developed formulation was anticipated to have desired PS, low PDI, and high EE. Based on the independent variables, namely concentration of solid lipids (2 – 3 %w/v), surfactant concentration (3 – 5 %v/v), and sonication time (100 – 200 sec) incorporated in the CCRD, 20 runs were suggested that were required to be prepared. These independent factors shown in Table 4 were used, and their impact on the dependent factors (PS and EE) was observed. These values of independent factors were selected based on the hit and trial method.

## 2.4. Characterization of optimized MG-SLNs

### 2.4.1. Particle size and PDI

These parameters were evaluated by Zetasizer (Malvern Zetasizer, Nano ZS, Ltd., UK) equipped with Malvern software (ver. 7.12). Particle size was reported by the equipment based on dynamic scattering. The dilution was done up to 10 times with the help of Milli Q water to obtain uniformly dispersal and thereafter evaluated at 90° at 25 ± 2 °C (Wu et al., 2020).

### 2.4.2. Entrapment efficiency (EE)

The developed MG-SLNs were centrifuged at 15,120 g force using Sigma-3 K30, Osterode am Harz, Germany, for approx. 30 min at 25 ± 2 °C. Later the supernatant obtained was taken for evaluation of the MG entrapped in the formulation. The sample was then diluted using methanol, then filtering using a 0.25 µm membrane filter. The filtrate solution being evaluated for MG via a UV spectrophotometer at 439 nm (Philip, 2011). The quantity of MG entrapment was determined by the below equation:

$$EE\% = \frac{(W_x - W_y)}{W_z} \times 100 \quad (1)$$

Here,  $W_x$  denotes the overall quantity of MG,  $W_y$  denotes the quantity of MG in the supernatant, and  $W_z$  denotes the mass of the lipid (Khan et al., 2016).

### 2.4.3. Zeta potential

This parameter was estimated by Zeta-sizer (Malvern Instruments, UK) based on the electrophoretic mobility of nanoparticles under the influence of an electric field. The solution was diluted by utilizing Milli Q water, followed by adding them into the chamber (Iqbal et al., 2021; Loo et al., 2013).

### 2.4.4. Surface morphology

Developed MG-SLNs preparation was evaluated by performing Transmission Electron Microscope (TEM) Morgagni 268 D. One droplet of the preparation was transferred on the carbon coated grid. After dried, the negative-staining was done by 1 % PTA (phosphor tungstic acid). Then the copper grid of the TEM was analyzed for the shape of the MG-SLNs (Philip, 2011).

### 2.4.5. In-vitro release parameter

The analysis was carried out with the help of dialysis pouch having molecular weight of 12–14 kDa. The 4 ml of MG-SLNs and MG-SOL were placed in the dialysis membrane containing MG equivalent to 75 mg, followed by placing it in the 0.1 N HCl and phosphate buffer saline of pH 7.4 that was then stirring on the magnetic stirrer kept at 37 ± 0.5 °C.

Later the solution (2 ml) being taken out at mentioned time intervals such as 0.5, 1, 2, 4, 8, 12, 24, and 48hr simultaneously and was then exchanged with the equal quantity of the respective buffer to keep the sink condition. The obtained solution was then diluted and evaluated for quantification of the MG in both media at 439 nm. The below-mentioned equation was used to calculate the % cumulative drug release. Later the release process was again evaluated via a fitting them in the several release kinetic parameters, namely first order, zero order, Higuchi and Peppas Korsmeyer arithmetical parameters (Weng et al., 2020).

$$\%Drug\ release = \frac{Conc.(\mu g/ml) \times DF \times Vol.of\ release\ medium(ml)}{Initial\ dose(\mu g)} \times 100 \quad (2)$$

Here, DF = Denotes dilution factor (Qamar et al., 2021).

### 2.4.6. Ex-vivo permeation study using intestinal segment

This study was carried out by replacing the dialysis membrane with the intestinal segment of male Wistar rats weighing 250 gm. The intestinal segment of the sacrificed rat was removed and cleaned using Tyrode's liquid to eradicate all the excretory products that were available in the duodenum. The intestinal duodenum part with a length of 9.6

± 0.6 cm and diameter of 2.56 ± 0.31 mm was filled with the formulation and solution of the MG separately comprising 75 mg of the MG in 10 ml of SLNs preparation and SOL separately (Kothari and Rajagopalan, 2020). This filled segment was then placed in 100 ml of the PBS (pH 7.4) that was kept at 37 ± 0.5 °C and shaken at 100 rpm on a magnetic stirrer. So, at numerous time-points 0.5, 1, 2, 4, 8, 12, 24, and 48 hr, the 2 ml solution was taken out from the diffusion medium followed by the addition of the same volume of fresh buffer to maintain sink conditions. All solution was estimated at 439 nm by UV-spectroscopy for the release of MG (Ahmad et al., 2018). The permeability coefficient was evaluated via a below equation:

$$Permeability\ coeff. (P_{app})(cm/sec) = \frac{dQ/dt}{A C_0} \quad (3)$$

Here, the proportion of permeable of MG is denoted by  $dQ/dt$ , cross-sectional area of the intestinal part by  $A$ , and  $C_0$  denotes the preliminary concentration instituted at  $t = 0$ .

### 2.4.7. Confocal laser scanning microscopy (CLSM)

This procedure was performed by filling up the intestinal segment with Rhodamine 123 (0.5 w/v) treated MG-SLNs and rhodamine hydro-ethanolic solution, follow up by the ligation at the end of the intestine and accomplishing it a sac. The intestine-filled sac was kept at 37 ± 0.5 °C in the Tyrode's liquid for 2 h followed by stirring at 50 rpm. After 2 h remedy, the ligated intestine was opened and rinse out with PBS (pH 7.4). This was then sent for the development of the slide. After the preparation of the slide, the intensity and the depth of penetration of the MG across the segment for 2 h was sensed via the z-axis by CLSM (LEICA TCS SPE) with LAS AF software (Alam et al., 2018).

### 2.4.8. Anti-oxidant using 2,2-diphenyl-1-picrylhydrazyl (DPPH) assay

The anti-oxidant efficacy of the MG-SLNs and MG-SOL was performed using DPPH assay by keeping ascorbic acid as the control. This detection was done on the capability of the DPPH to remove the free radicals. All these samples had their stock solution prepared (1 mg/ml) and were added in the methanol individually, follow up by dilution in the range 1–50 µg/ml.

Concurrently, adding together of the 1 ml of 200 µM DPPH solution was accomplished in every dilution (1 ml) of the individual sample. Every sample was then assessed after 30 mins for the absorbance at 515 nm by spectroscopy by using methanol as blank. The below equation was then applied to evaluate the % of inhibition;

$$\%Inhibition\ of\ DPPH\ radical = \frac{A_a - A_b}{A_a} \times 100 \quad (4)$$

Here, in the equation, Aa signifies the blank (control) i.e., ascorbic acid (AA) absorbance and Ab denotes the absorbance of the sample, respectively.

The graph was plotted between the mean % inhibition and the respective log concentration, which helped in the evaluation of the 50 % inhibitory dose (IC<sub>50</sub>) from the regressed equation (Leaves et al., 2014).

#### 2.4.9. Molecular docking study

The crystal structures of  $\alpha$ -glucosidase (5NN6),  $\alpha$ -amylase (5E0F), PTP1B (2ZMM), and DPP-IV (2G63) were taken from the protein data bank. These protein structures were made by Protein preparation wizard in Maestro interface of Schrodinger suite 2021–2. In this step bond order assignment, addition of polar hydrogens, addition of formal charges on metal ion, prediction of ionization state, tautomeric states, and finally restrained minimization of the entire protein was carried out. Receptor grid was generated by placing a cubical shaped grid keeping the co-crystallized ligand as the centroid (Mahapatra et al., 2014).

Mangiferin and Acarbose structures were drawn and then prepared using LigPrep module (Schrodinger, 2021) where polar hydrogens were added, tautomers were generated and finally they were energy minimized. Low energy conformations of these structures were selected for extra-precision (XP) docking against 5NN6, 5E0F, 2ZMM, and 2G63 respectively. The XP docking were applied by Glide module of Schrodinger suite 2021–2 where a single best pose was generated and the final assessment was done according to the Glide docking score (Friesner et al., 2004; Friesner et al., 2006).

#### 2.4.10. Alpha ( $\alpha$ ) – Amylase inhibitory assay

This method was performed using the dinitrosalicylic acid (DNS) method. In this procedure, a stock solution (100  $\mu$ g/ml) of MG was prepared, out of which different solutions were prepared, including (25,50,100 & 200  $\mu$ g/ml) and acarbose (100  $\mu$ g/ml) that was incubated with 1 ml of the  $\alpha$ -amylase (this was diluted for approx. 10 k in 20 mM of the sodium PBS (pH 6.9) for about 30 min before the addition of the starch solution (1 ml of 1 %w/w) of the starch solution). Later this combination was incubated at  $37 \pm 0.5$  °C for about 15 mins. The reaction then stopped on adding 1 ml DNS reagent, and then the obtained contents was heat up in the bubbling water bath for 5 mins. The control was developed without using the sample (Ac) and blank, which was without  $\alpha$ -amylase (Ab). So, the absorbance was evaluated at 540 nm by UV spectrophotometer. The reference that was used for this procedure was acarbose. Later the % inhibition was estimated by the below-mentioned equation (5) (Ngo et al., 2019).

$$\text{Inhibition (\%)} = [(A_c - A_b) - (A_{\text{sample}} - A_b)] / (A_c - A_b) * 100 \quad (5)$$

### 2.5. Here a stands for the respective absorbance

#### 2.5.1. Alpha ( $\alpha$ ) – Glucosidase inhibitory assay

In the  $\alpha$ -glucosidase inhibitory assay, a total of 120  $\mu$ L of the test sample and 20  $\mu$ L of  $\alpha$ -glucosidase solution (with an activity of 1 U/mL in a 0.1 M potassium phosphate buffer at pH 6.8) were combined and placed in a 96-well plate. This mixture was then incubated at 37 °C for 15 min. Subsequently, 20  $\mu$ L of a solution containing *para*-nitrophenyl- $\alpha$ -D-glucopyranoside (5 mM) was added to initiate the reaction, and incubated for an additional 15 min. To stop the reaction, 80  $\mu$ L of a 0.2 M sodium carbonate solution was utilized, and the resulting solution was analyzed spectroscopy at 405 nm. Acarbose served as the positive control in this assay (Mahapatra et al., 2014; Schrödinger, 2021; Friesner et al., 2004). Later the % inhibition was estimated by the below-mentioned equation (6).

$$\text{Inhibition (\%)} = [(A_c - A_b) - (A_{\text{sample}} - A_b)] / (A_c - A_b) * 100 \quad (6)$$

### 2.6. Here a stands for the respective absorbance

#### 2.6.1. Induction of diabetes

Induction of diabetes in albino rats through a combination of a maximum fat diet and a single intra-peritoneal delivery of a low dose of streptozotocin (35 mg/kg). After 72 h of streptozotocin delivery, the fasting blood glucose level (BGL) was determined using a digital glucometer (Accu Check, Roche, Germany). Rats with fasting BGL levels same or higher than 220 mg/dL were considered to be in a diabetic condition and were included in the experimental study.

#### 2.6.2. Evaluation of anti-diabetic activity

The study was conducted following the previously reported study (Friesner et al., 2006; Trinder, 1969). The study included four groups:

Group-1: Served as the normal control.

Group-2: Was designated as the disease control.

Group-3: Received treatment with MG-SLNs.

Group-4: Received treatment with MG-SOL.

In groups (3) and (4), animals were taken orally with MG equivalent to 40 mg per kilogram of body weight. Blood glucose levels were assessed at mentioned time intervals such as 0, 1, 2, 4, 8, 12, and 24 h using a digital Accu-Check glucometer. Small blood sample was obtained from the rat's tail and placed on a glucometer strip. The blood glucose level was displayed on the glucometer screen and recorded. This evaluation was conducted for up to 24 h, and the %reduction in BGL was estimated using the provided equation.

$$\% \text{Reduction in BGL} = \frac{BGL_{t=0} - BGL_{t-1}}{BGL_{t=0}}$$

#### 2.6.3. Biochemical study

Following the completion of the study, blood solutions were obtained from the *retro*-orbital plexus of the animals while under anesthesia induced by a light dose of diethyl ether. These blood samples were permitted to stand undisturbed for 30 min and were then centrifugated at 3000 revolution per minutes till 15 min. Resulting clear supernatant, which is the blood serum, was split and stored in a refrigerator at temperatures between 2 and 4 °C. This blood serum was later used for conducting liver function tests, including SGOT and SGPT, as well as a lipid profile analysis, which included measurements of cholesterol, triglycerides, and HDL (Trinder, 1969).

#### 2.6.4. Statistical analysis

The data presented in the manuscript have been statistically analyzed by Graph-Pad Prism software (GraphPad 9.0, San Diego, USA). All the data are presented as mean  $\pm$  SD. The statistical implications were established at  $p < 0.05$  until mentioned.

## 3. Results

### 3.1. Assortment of solid lipids and surfactant

The highest soluble of MG was obtained in the Labrafil M 2130 CS (77.63  $\pm$  5.78 mg/g), as shown in Fig. 1 (a) in comparison to the other lipids due to the self-emulsifying characteristic of the solid lipid that will further assist in enhancing the bioavailability of the MG at the required site thus upsurging the oral bioavailability (Zhang et al., 2021). Whereas, in the case of surfactants, Tween 80 offered the highest solubility for MG, i.e., 35  $\pm$  3.74 mg/ml, as shown in Fig. 1 (b). Tween 80 is a non-ionic surfactant which is safe for human use due to fewer toxicity issues (Varshosaz et al., 2010).

### 3.2. Formulation composition optimization

On putting independent and dependent factors in the CCRD design, 20 runs came up, and according to these runs, various formulations were

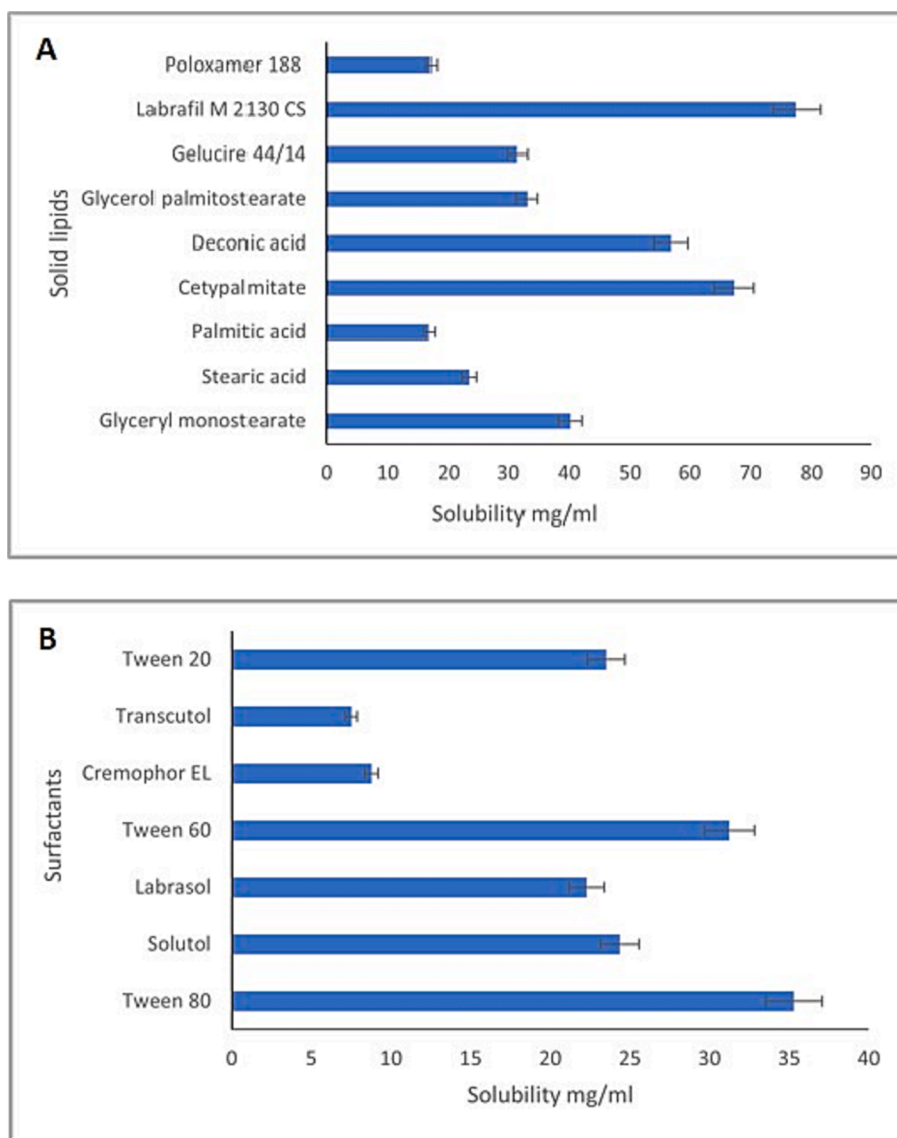


Fig. 1. MG-solubility, A. MG solubility in various solid-lipids, B. MG solubility in various surfactants.

developed. These developed preparations were being assessed for PS and EE. These factors have been mentioned in Table 1.

### 3.3. Response surface exploration

#### 3.3.1. Effect of independent factors

**3.3.1.1. Particle size.** The observed PS values of the developed MG-SLNs were found to be in the series of 181.42 to 38.97 nm. The quadratic equation so obtained presented a highly significant effect ( $p < 0.0001$ ) of the solid lipid, surfactant concentration, and sonication time on the PS values. It is probable that an upsurge in the amount of solid lipids will directly consequence in a rise in the formulation's particle size (Gaba et al., 2015). Whereas a rise in the quantity of surfactant leads to drop in the PS because of the drop in the interfacial surface tension between the lipidic part and hydrophilic part (Varshosaz et al., 2010; Gaba et al., 2015). Additionally, because the SLNs formulations' particles were broken up during the sonication process, the particle size was also reduced. Fig. 2(a) shows the effect of these independent variables in combination with the PS. The amount of both solid lipid and surfactant in combination displayed a negative impact. Similarly, surfactant concentration and sonication time in combination displayed a negative

impact on the PS. But, on the contrary, the sonication time and surfactant amount showed a positive impact on the particle size.

Particle size (R1) =  $93.87 + 37.76^*A - 13.20^*B - 24.68^*C - 5.91^*AB - 1.10^*AC + 0.42^*BC + 4.97^*A^2 - 3.99^*B^2 + 6.31^*C^2$ .

**3.3.1.2. Entrapment efficiency.** The EE of all the runs obtained was found to be in the limit of 52.22 to 92.54 %. The impacts of the independent levels on the EE of the MG in SLNs was found to be highly significant  $< 0.0001$ , which caused an increase and decrease in the EE. According to the quadratic polynomial equation obtained, the increment in the amount of the solid lipid resulted in an upsurge in the EE due to the entrapping of the drugs in large amounts (Behbahani et al., 2017). Also, the rise in the amount of the surfactant caused a rise in the EE of the MG due to the manifolds of the layers of surfactant around the particle of the formation (Keum et al., 2011). Moreover, Tween 80 has a high probable to increase the solubilization of the drug. In addition, the increase in the sonication time increased the encapsulation efficiency of the MG efficiently (Üner and Yener, 2007). The particles that would further entrap additional MG are broken when the sonication period is extended. The combined impact of the independent factors on the EE is also viewed in Fig. 2(B). Due to the high MG entrapment, the mixture of solid lipid content and surfactant has a beneficial effect on EE. A

**Table 1**

Formulations, evaluated for particle size and entrapment efficiency.

Runs	-Solid lipid concentration (A; % w/w)	Surfactant (B; % v/w)	Sonication time (C; sec)	PS (nm)	EE (%)
1	4	3	100	181.42	92.54
2	1.31	4	150	43.14	53.54
3	3	4	234.09	67.39	66.45
4	3	4	150	95.04	85.05
5	4	3	200	132.42	80.22
6	3	4	65.91	151.54	87.33
7	4.68	4	150	168.21	93.98
8	3	5.68	150	50.72	70.98
9	4	5	200	98.34	77.43
10	2	3	100	94.01	76.55
11	3	2.31	150	109.95	85.02
12	3	4	150	93.44	84.98
13	3	4	150	95.83	84.87
14	2	3	200	43.55	61.09
15	4	5	100	151.52	82.24
16	3	4	150	93.23	86.07
17	3	4	150	94.34	86.12
18	3	4	150	92.11	85.44
19	2	5	100	81.87	72.54
20	2	5	200	38.97	54.22

detrimental result was obtained when solid lipid concentration and sonication time were combined with surfactant concentration and sonication time.

$$EE (R2) = 83.25 + 11.63*A + 0.57*B + 0.25*C + 0.39*AB - 0.29*AC - 0.48*BC - 2.95A^2 + 2.31B^2 - 6.31C^2$$

**3.3.1.3. Design validation.** The CCRD was used to attain the preparation with optimum PS and EE. The values that have been predicted of all the responses and factors. Hence, MG-SLNs were then formulated depending on the run and process variables and responses. In addition, the experimental and predicted values were observed to similar, thereby demonstrating the authenticity of the optimisation process.

### 3.4. Optimized formula for the development of MG SLN

After applying CCRD, the optimized MG SLNs were prepared by taking 3 % w/v solid lipid mixture and 4 % v/v of the concentration of surfactant, followed by sonication for 150 sec. The MG developed was mixed in the lipidic phase to encapsulate the drug, follow up by the adding of ethanol. Then, the aqueous phase was developed, followed by mixing with the lipidic phase. This was then subjected to sonication for 150 sec to obtain MG SLNs. This developed formulation was then characterized by various characteristic features (Behbahani et al., 2017).

### 3.5. Characterization of optimized MG SLN

#### 3.5.1. PS and PDI

The developed optimized MG SLN formulation exhibited a PS of  $138.37 \pm 3.39$  nm and PDI of  $0.247 \pm 0.023$ , as presented in Fig. 3. The PS obtained of MG loaded SLN is best suited for the development of the formulation for oral administration as it is in the limited range (Üner and Yener, 2007). Thus, releasing the MG at the desired site could ultimately lead to the modulation of diabetes militias. Moreover, the PDI obtained showed that the developed formulation fell under the range of 0.0 to 1.0, signifying that the formulation didn't possess any kind of aggregation, suggesting its stability and uniformity (Danaei et al., 2018).

#### 3.5.2. EE

EE of MG-SLNs was obtained to be  $84.37 \pm 2.43$  %, signifying that this amount of the MG got entrapped in the solid-lipid and surfactant that have been employed in the formulation development (Mahajan and

Patil, 2021).

#### 3.5.3. Zeta potential

The mean ZP of the developed formulation MG-SLNs is observed to be  $18.87 \pm 2.42$  mV, as presented in Fig. 4. As this value of ZP falls under the range of  $< -25$  mV or  $> +25$  mV, it can be well seen that the obtained value lies very close to  $+25$  mV; therefore, it can be so, it can be well understood that the developed formulation is very much near to stability. This value of ZP further specifies that the optimized formulation lacks any existence of aggregation (Madan et al., 2014).

#### 3.5.4. Surface morphology

The shape of MG-SLNs was examined using TEM, as shown in Fig. 5, where it can be seen that the particles were spherical in shape in developed formulation having black borders and size less than 200 nm. The image helps in demonstrating that the loaded MG is well encapsulated in the lipid followed by outer covering by the layer of surfactant (Imran et al., 2020).

#### 3.5.5. In-vitro release analysis

The % cumulative quantity of MG released from MG-SLNs and MG-SOL in 0.1 N HCl was observed to be  $79.12 \pm 4.87$  % and  $37.26 \pm 2.99$  %, respectively. In PBS (pH 7.4), it was found to be  $80.21 \pm 5.61$  % and  $36.07 \pm 3.04$  %, respectively (Fig. 6). The initial release of the MG in large amounts from formulation could be due to the entrapped MG in the lipidic layer of the SLNs. This factor is further accountable for the sustained release model of the MG from the preparation. Moving of the aqueous part in the core of the SLNs resulted in the dissolution of the MG that caused the increase in the % release. Moreover, the presence of the surfactant in higher concentrations and the leaky nature of the SLNs augmented the releasing efficiency of MG in comparison to that of the SOL.

Various models were used, as depicted in Figs. 7 and 8, to evaluate the kinetic release of the MG from MG-SLNs in both the media, namely 0.1 N HCl and PBS (pH 6.4); it was discovered from these models that the release of the MG from formulation followed Higuchi model in 0.1 N HCl whereas, Korsmeyer Peppas model was followed in PBS (pH 7.4). These models were the best-fitted models as the values of  $R^2$  were found to be highest amongst others in both the media. Moreover, in PBS (pH 7.4), the 'n' value was found to be 0.32, which is  $< 0.43$ , so it can be suggested that the release of the MG from MG-SLNs in PBS followed Fickian diffusion (Jazuli et al., 2019).

#### 3.5.6. Ex-vivo permeation study using intestinal segment

The permeation profile of the MG from the formulation and SOL was evaluated using an intestinal membrane. The permeability coefficient was found to be  $4.87 \times 10^{-3}$  cm/s when compared to SOL which was found to be  $2.82 \times 10^{-3}$  cm/s after 2 h, as shown in Fig. 9. In contrast, a 4-times rise in the permeable of MG from SLN and SOL was observed within 2hr. In addition, a 2-times enhancement was found in the flux from MG-SLNs ( $36.53 \mu\text{gcm}^{-2} \text{h}^{-1}$ ) in comparison with the MG-SOL ( $21.91 \mu\text{gcm}^{-2} \text{h}^{-1}$ ). This significant change in the permeation of MG from SLNs could be because of the presence of the permeation enhancer, i.e., Tween 80. Moreover, the nano-size of the formulation contributed to the permeation, thus enhancing the permeation profile of the SLNs.

#### 3.5.7. CLSM study

This method was implemented to estimate the permeation potential of the MG from SLNs in comparison to rhodamine hydro-ethanolic solution across the intestinal segment. According to the images as shown in Figure 10, it can be well understood the formulation treated with dye was able to permeate deeper, i.e., 30  $\mu\text{m}$ , in comparison to the rhodamine hydro-ethanolic solution. This could become possible because of the available of the permeable enhancer, namely Tween 80, and the nano-sized formulation, thus resulting in deeper permeation of due treated formulation thus, highlighting the emphasis of this study.

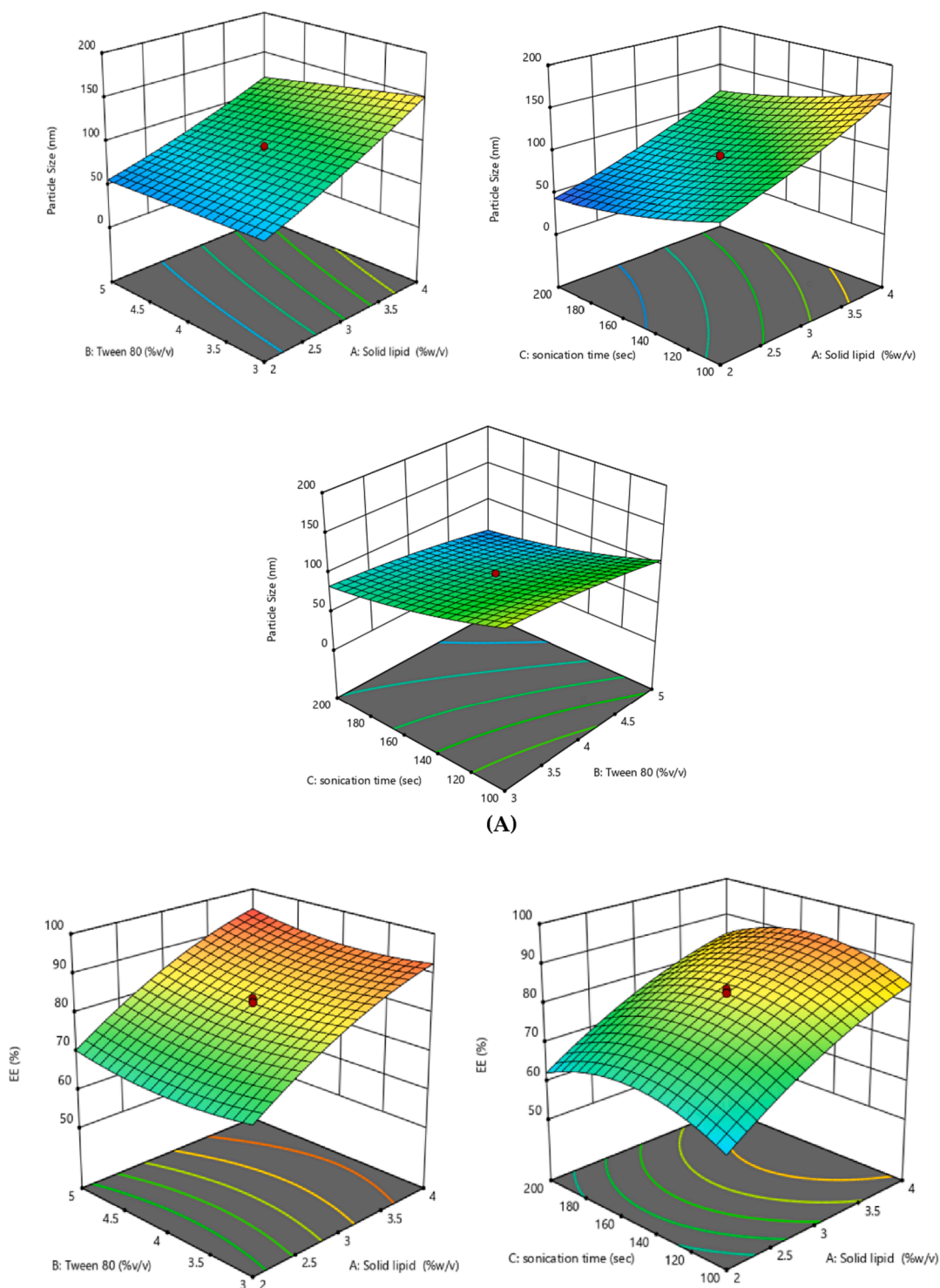


Fig. 2. Effect of variables on A. PS and B. EE.

### 3.5.8. Anti-oxidant activity

The reducing characteristic of DPPH caused by antioxidants was evaluated by the decrease in the absorbance at 515 nm, which was determined by the alteration in colour from violet to colorless. The result obtained, as shown in Fig. 11, showed a major decrease in the DPPH radical amount that was brought by MG-SLNs than MG-SOL. There was an increase in the antioxidant activity of MG-SLNs at 60  $\mu\text{g}/\text{mL}$  than the MG-SOL; that could be due to the collective effect of the MG and the surfactant as; both are antioxidants in nature. However, the  $\text{IC}_{50}$  value of

the AA, MG-SOL, and MG-SLNs were observed to be 23.33  $\mu\text{g}/\text{mL}$ , 49.08  $\mu\text{g}/\text{mL}$ , and 46.14  $\mu\text{g}/\text{mL}$ , accordingly (Thaipong et al., 2006). However, different studies have been conducted, which has significantly explained the anti-oxidant properties of the MG either in free form or in formulation (Dar et al., 2005; Samadarsi and Dutta, 2019; Donga and Chanda, 2021).

### 3.5.9. Targets and molecular docking

Mangiferin is a C-glucosyl xanthone with a polyphenolic structure.

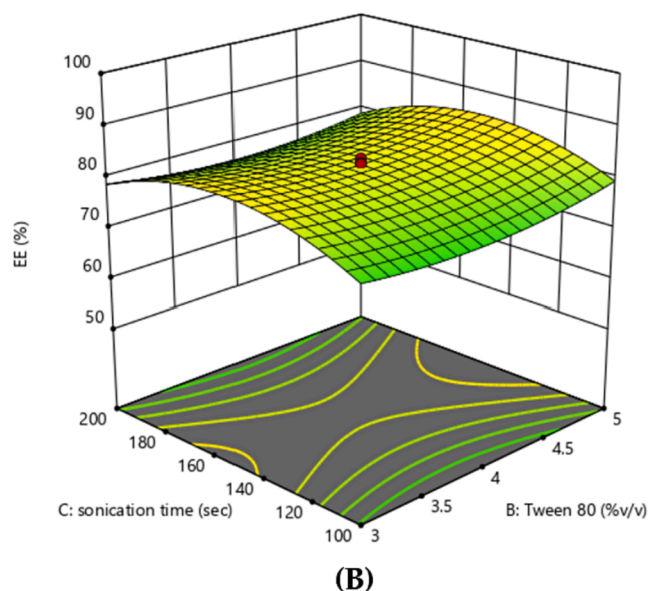


Fig. 2. (continued).

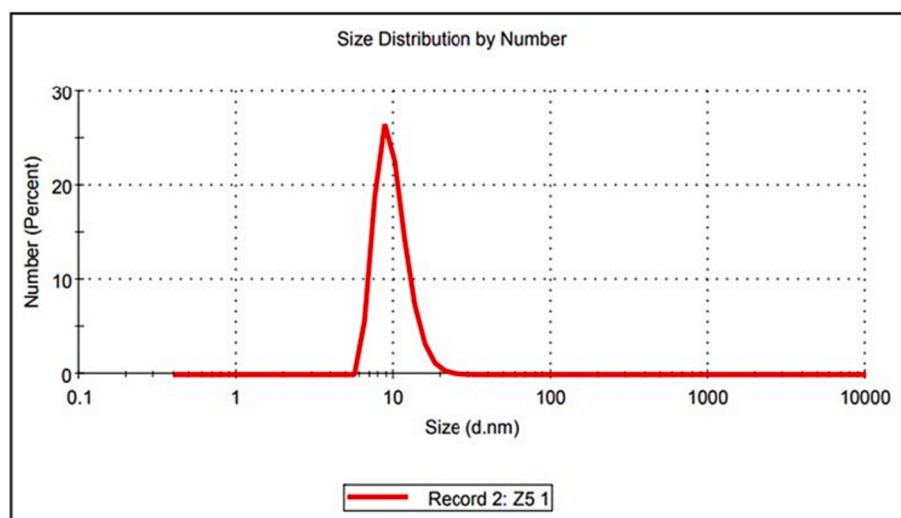


Fig. 3. PS and PDI of MG-SLNs optimized formulation.

The xanthone nucleus forms a glycosidic bond with the glucose. The benzene rings of the xanthone nucleus are essential and responsible for the hydrophobic contacts, whereas the peripheral (substituted) hydroxyl groups are involved in forming hydrogen bonds. Phenolic OH groups of the glucose are responsible for H-bond formation with hydrophilic residues like ASP197 and GLH (Glu) 233. Phenolic OH at C-7 of the terminal benzene ring was found to be involved in forming H-bonds with ASP356 residue. Both the terminal benzene ring and its adjacent pyran nucleus form hydrophobic links with residue TRP59 through pi-pi contact.

Mangiferin has been reported to be inhibitors of various enzymes like  $\alpha$ -Glucosidase,  $\alpha$ -Amylase, protein tyrosine phosphatase-1B (PTP1B), and dipeptidyl peptidase 4 (DPP-IV), which are responsible for causing type 2 diabetes. To test the binding affinity of mangiferin towards these enzymes, mangiferin was docked against 5NN6 ( $\alpha$ -glucosidase), 5E0F ( $\alpha$ -amylase), 2ZMM (protein tyrosine phosphatase-1B), and 2G63 (dipeptidyl peptidase). Acarbose was also docked against these four enzymes as a reference standard drug. The docking scores of acarbose and mangiferin represented in Table 2. Acarbose was having higher docking scores than mangiferin against all the four enzymes. Mangiferin

has shown docking score of  $-10.057$  against 5E0F,  $-8.096$  against 5NN6,  $-7.454$  against DPP-IV, and  $-6.301$  against 2ZMM. Docking study results revealed that mangiferin has got the highest binding affinity towards  $\alpha$ -amylase (5E0F) protein structure in comparison to other three enzymes. Some previous studies have also shown high binding affinity of mangiferin against  $\alpha$ -Amylase (Picot et al., 2017). The findings of the docking study led us to conduct mangiferin formulations mediated *in-vitro*  $\alpha$ -amylase activity, the results of which have been presented in the next section. Fig. 12 depicts the two-dimensional (2D) interaction diagram of mangiferin against 5E0F where different interactions made by the interacting residues of the active site of  $\alpha$ -amylase protein has been shown.

#### 3.5.10. Alpha ( $\alpha$ ) – Amylase inhibitory assay

$\alpha$ -amylase is known to be the utmost crucial digestive enzyme that is responsible for the hydrolysis of  $\alpha$  – 1,4glycosidic linkages of the carbohydrate. It further breaks the large molecules of starch into tiny fragments of sugar to cross the epithelium of the gut. Therefore, the inhibition of the  $\alpha$ -amylase activity would decline the postprandial hyperglycemia that would ultimately prevent the risk of development of

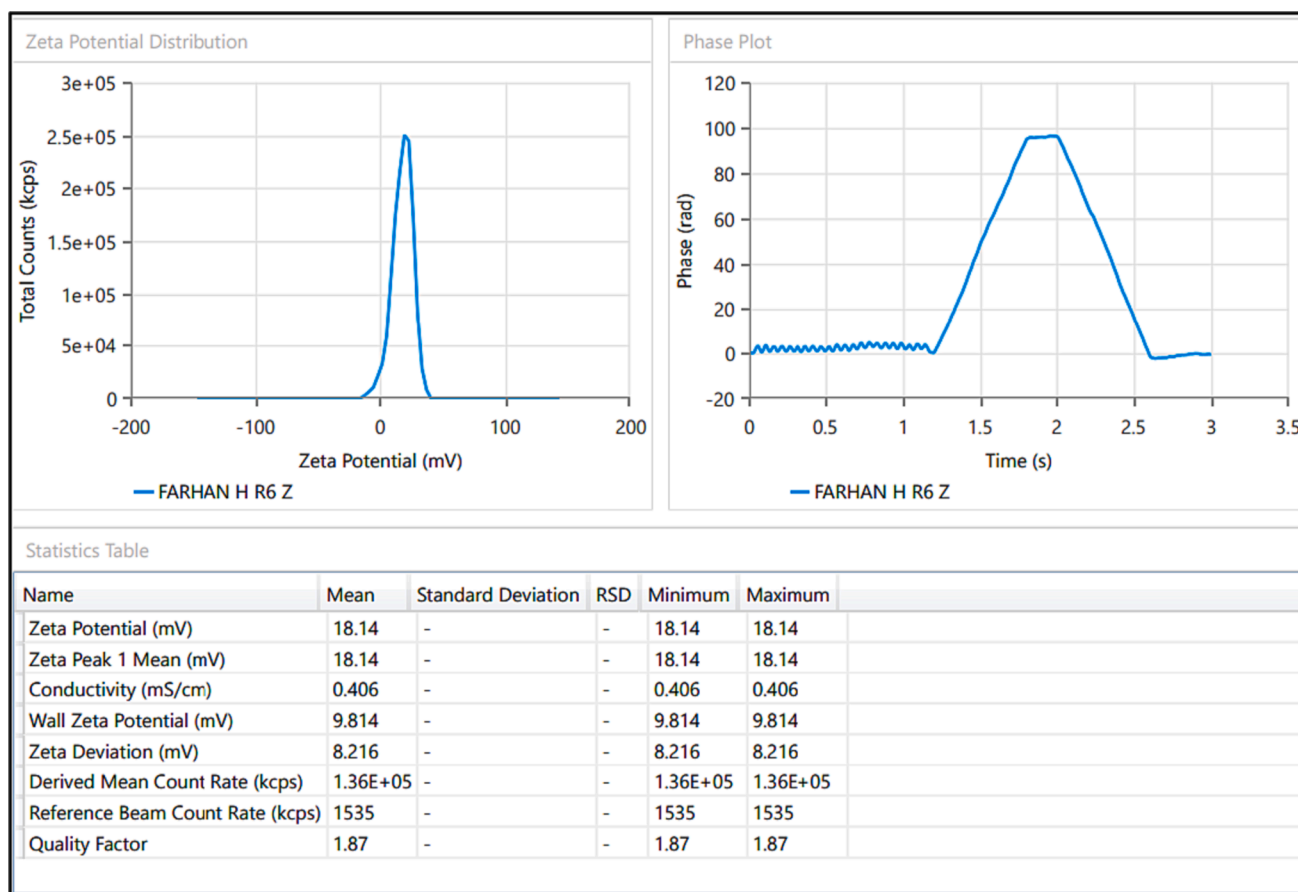


Fig. 4. ZP of the optimized MG-SLNs.

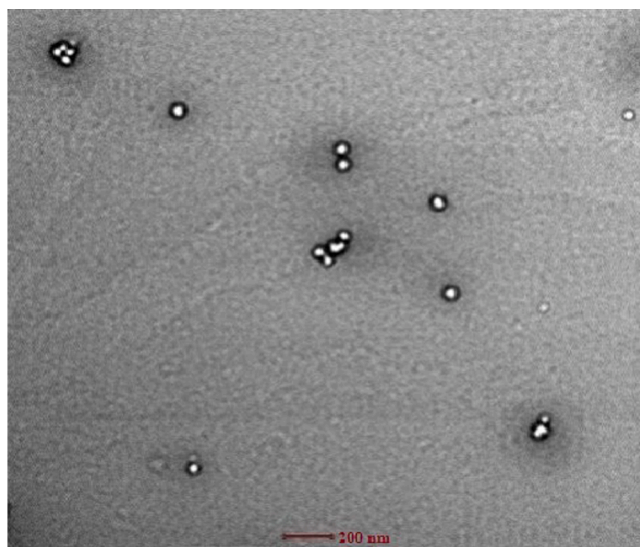


Fig. 5. TEM image of the optimized MG-SLNs.

diabetes. Therefore, in this study, the capacity of MG against  $\alpha$ -amylase activity was evaluated. The results obtained showed that MG-SLN was highly significant in reducing the  $\alpha$ -amylase activity in a dose dependent approach, as shown in Fig. 13. The inhibitory effect of MG-SLN and MG-SOL was found to be  $55.43 \pm 6.11\%$  and  $51.71 \pm 6.02\%$  at  $100 \mu\text{g}/\text{mL}$ , but acarbose showed inhibitory effect of  $78.01 \pm 7.45\%$  at  $100 \mu\text{g}/\text{mL}$ . Therefore, it can be predicted that the inhibitory activity of the MG in SLN is moderate in comparison to SOL (Ngo et al., 2019; Jazuli et al.,

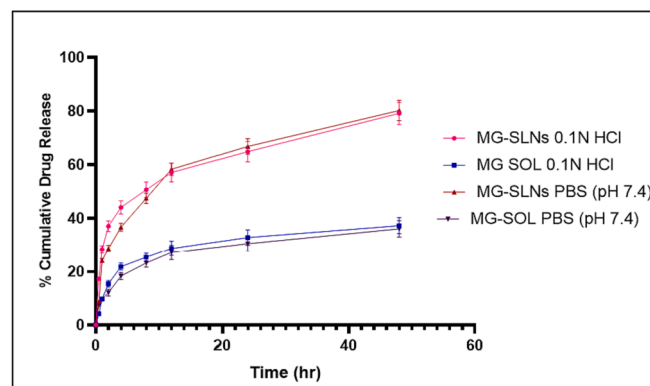


Fig. 6. Release study of MG from MG-SLNs and SOL in 0.1 N HCl and PBS (pH 7.4).

2019). Parallel to this, different studies have shown the enzyme inhibitory nature of MG, in which MG significantly reduced the activity of the  $\alpha$ -amylase thus, acting against diabetes (Sekar et al., 2019).

### 3.5.11. Alpha ( $\alpha$ ) – Glucosidase inhibitory assay

The enzyme  $\alpha$ -glucosidase plays an imperative role in diabetes regulation, and it's commonly assessed using the enzyme-substrate reaction method, a broadly accepted method in anti-diabetic studies (Capetti et al., 2020; Gaurav et al., 2020; Tahir et al., 2016). In our current research, we evaluated the inhibitory effect of MG-SLNs on  $\alpha$ -glucosidase, following the standard enzyme-substrate reaction protocol. Additionally, we compared the results to acarbose. Our findings

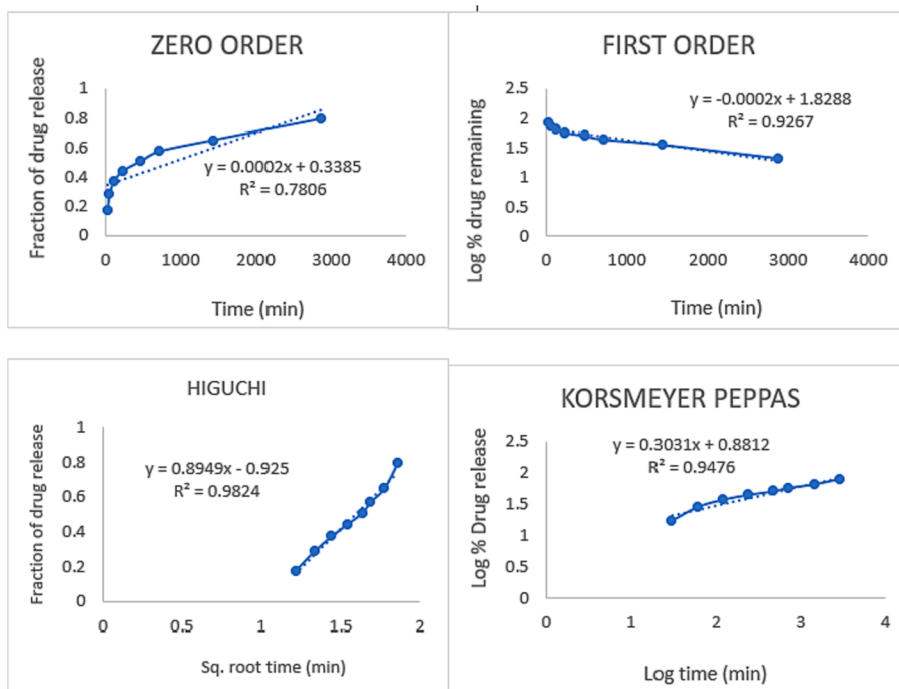


Fig. 7. Release profile of MG from MG-SLNs formulation by different models in 0.1 N HCl.

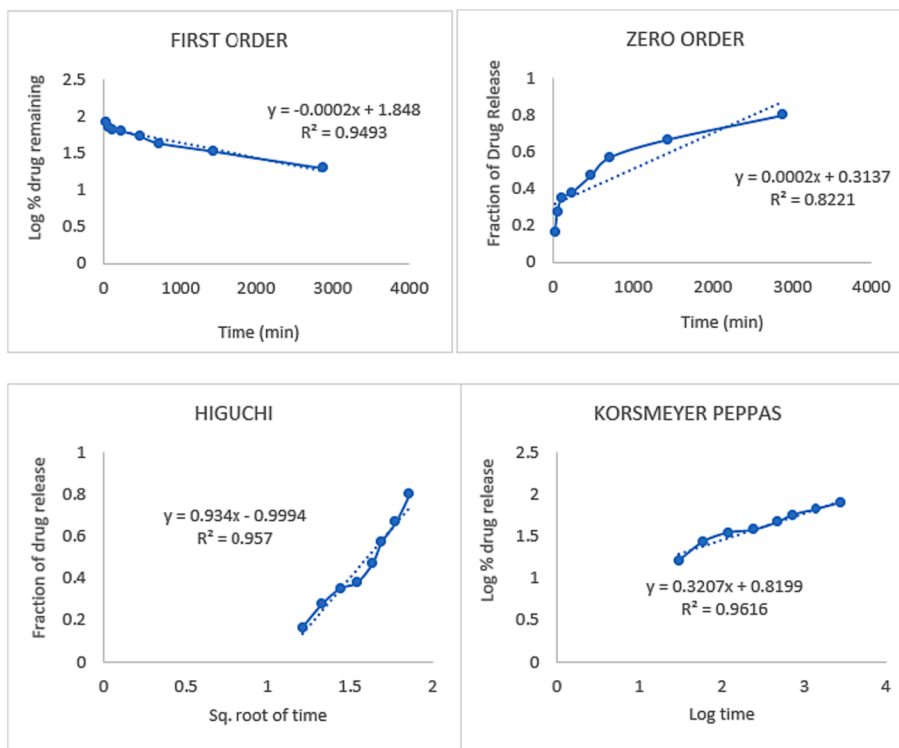


Fig. 8. Release profile of MG from MG-SLNs formulation by different models in PBS (pH 7.4).

indicate that MG-SLN exhibited a remarkable  $\alpha$ -glucosidase inhibition of  $68.76 \pm 3.14$  %, whereas acarbose displayed an inhibition of  $63.43 \pm 4.02$  %. Notably, MG-SLNs demonstrated a significant and even higher inhibitory effect assessed to the control group treated with acarbose.

### 3.6. Assessment of anti-diabetic activity

In the study, the reasonable anti-diabetic effects of MG-SOL and MG-SLNs were assessed in Wistar rats with STZ-induced diabetes. The baseline BGL in the normal control (Group (1)) were measured at  $98 \pm 3$  mg/dL, while the diabetic control group (Group (2)) exhibited significantly elevated BGL at  $232 \pm 8$  mg/dL.

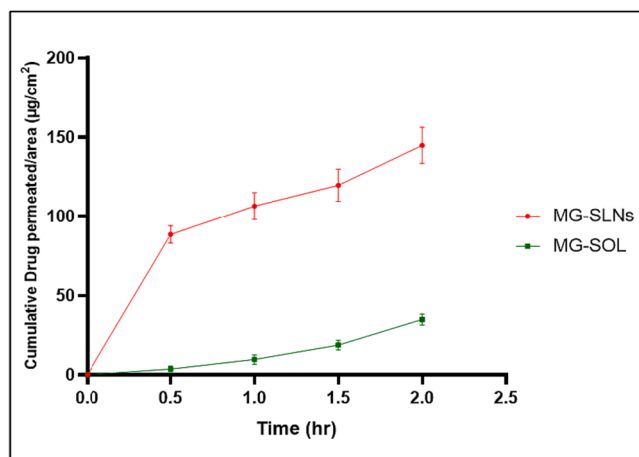


Fig. 9. Cumulative amount of MG permeated per area from MG-SLNs and MG-SOL across the intestine in PBS (pH 7.4).

Rats treated with MG-SLNs (Group (3)) exhibited a remarkable and sustained reduction in blood glucose levels (BGL) for up to 12 h. The most significant drop occurred in the MG-SLNs treated group, reaching  $116 \pm 4$  mg/dL, compared to the MG-SOL treated group (Group (4)), which showed a maximum reduction in BGL to  $131 \pm 5$  mg/dL. This suggests that MG-SLNs exhibited a significantly superior hypoglycemic

effect compared to MG-SOL, with a p-value less than 0.001.

These findings confirm that MG is more therapeutically effective when encapsulated in SLN formulation as shown in Fig. 14. The improved absorption of MG in the SLN preparation may be attributed to enhanced lymphatic drug transport. The external lipid-based formulation contributes to increased lymphatic transport by promoting the formation of lipoproteins and intestinal lymphatic lipid flux (Pandey et al., 2018; Arrua et al., 2021).

### 3.6.1. Bio-chemical study

In the analysis, serum biochemical considerations were assessed by standard kits. The levels of total cholesterol (TC) and triglycerides (TG) showed significant reductions ( $P < 0.001$ ), while high-density lipoprotein cholesterol (H-DLC) levels significantly increased ( $P < 0.001$ ) following treatment with both MG-SOL and MG-SLNs when compared to diabetic control rats (Table 3).

Furthermore, the levels of SGOT and SGPT were significantly reduced ( $P < 0.001$ ) after treatment with both MG-SOL and MG-SLNs in comparable to the diabetic control group. Notably, MG-SLNs exhibited a significant ( $P < 0.01$ ) reduction in serum SGOT levels compared to the MG-SOL-treated group.

These results suggest that both MG-SOL and MG-SLNs significantly improved the biochemical alterations associated with diabetes. The disruptions in insulin levels play a primary role in variations in the lipid profile, which can contribute to cardiovascular complications related to diabetes (Mersad Sefidgar et al., 2019). Moreover, due to the liver

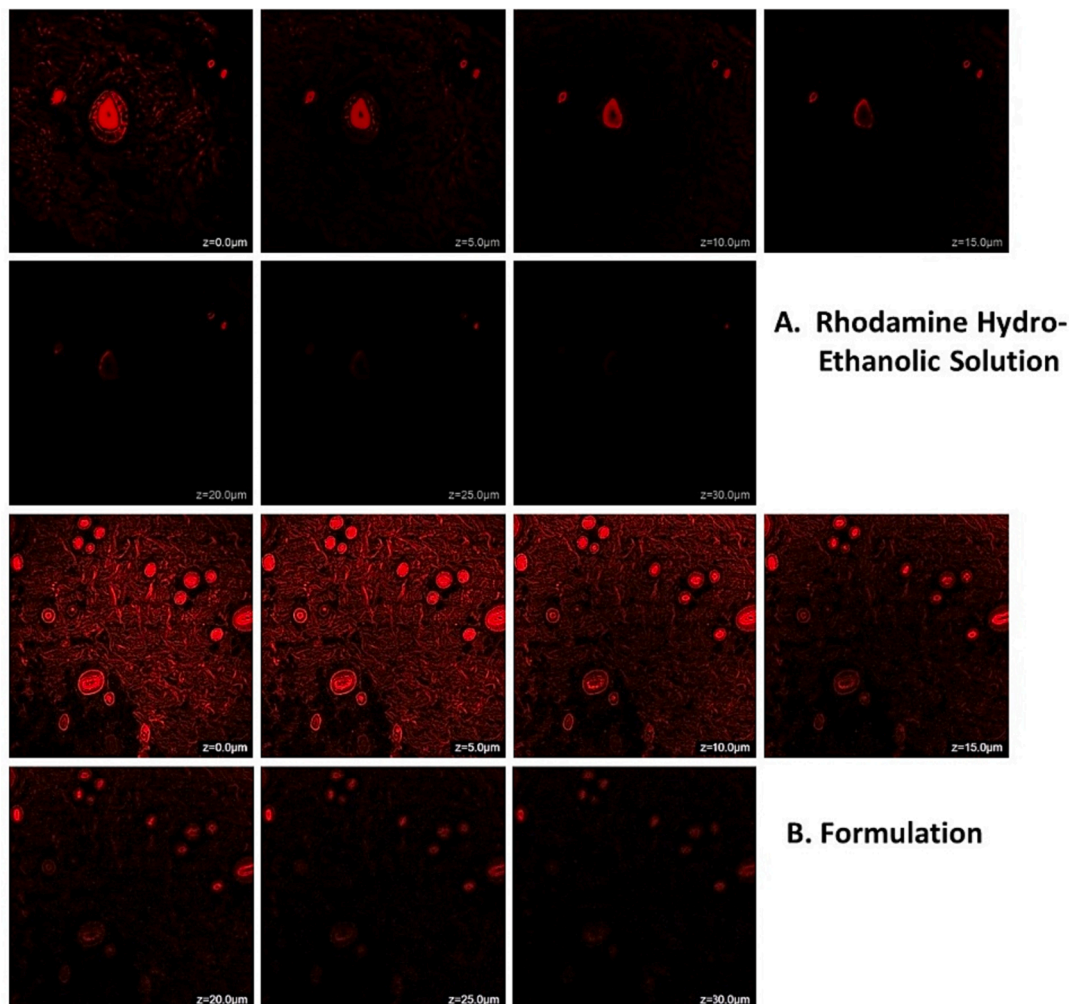


Fig. 10. Confocal images of the permeation of the MG-SLNs in comparison to a rhodamine-ethanolic solution.

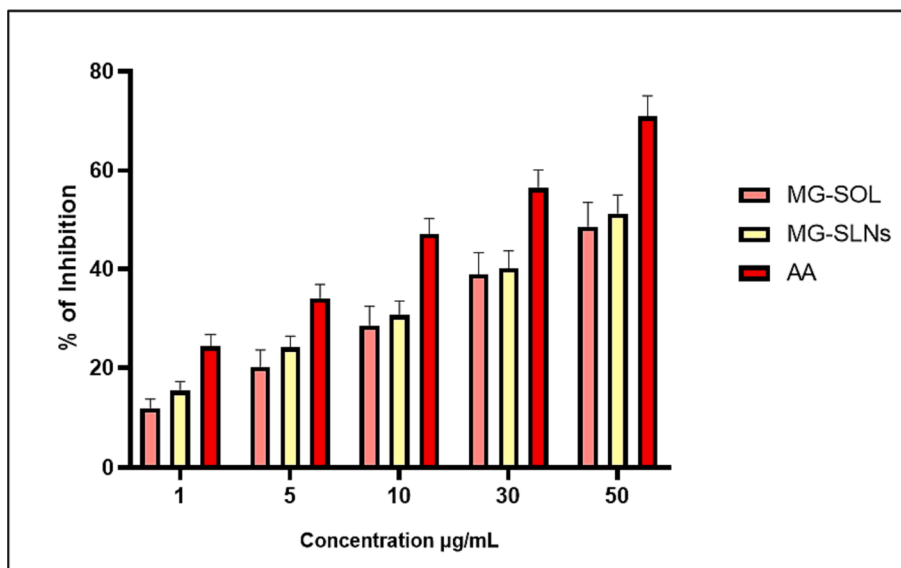


Fig. 11. Anti-oxidant activity of MG-SLNs in comparison to MG-SOL and AA (control).

**Table 2**  
Docking scores of mangiferin and acarbose.

Enzymes	Docking score	
	Mangiferin	Acarbose
α-glucosidase (5NN6)	-8.096	-8.819
α-amylase (5E0F)	-10.057	-14.869
PTP1B (2ZMM)	-6.301	-9.137
DPP-IV (2G63)	-7.454	-10.069

toxicity induced by STZ in rats, there is an excessive release of liver enzymes, and these levels were restored to normal values with MG-SLNs treatments (Nabi et al., 2013).

#### 4. Discussion

Among all the solid lipids screened for the solubility study of MG, the highest solubility was observed in Labrafil M 2130 CS due to the self-emulsifying characteristic of the solid lipid. whereas, amongst surfactants Tween 80 exhibited highest solubility. Tween 80 is a non-ionic surfactant which is safe for human use due to fewer toxicity issues. The observed PS values of the developed MG-SLNs were found to be in

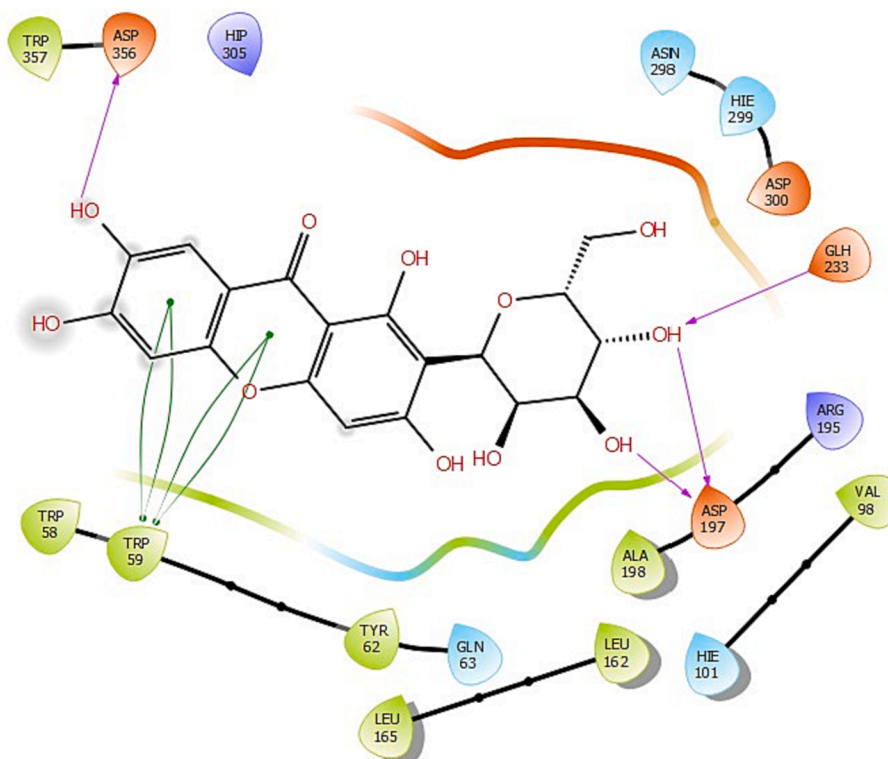


Fig. 12. Two-dimensional (2D) interaction diagram of mangiferin against 5E0F.

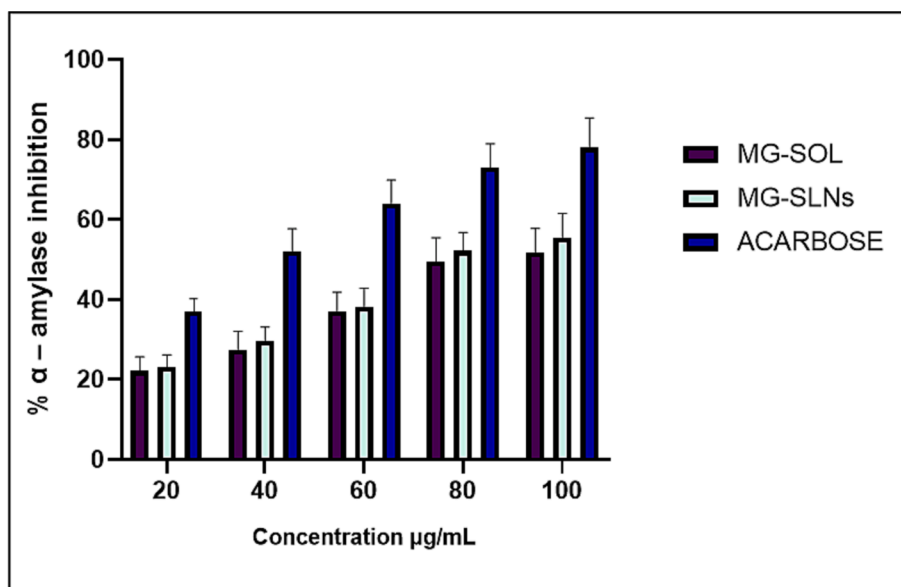


Fig. 13. α-amylase inhibitory activity of MG in SLNs and SOL in comparison to acarbose.

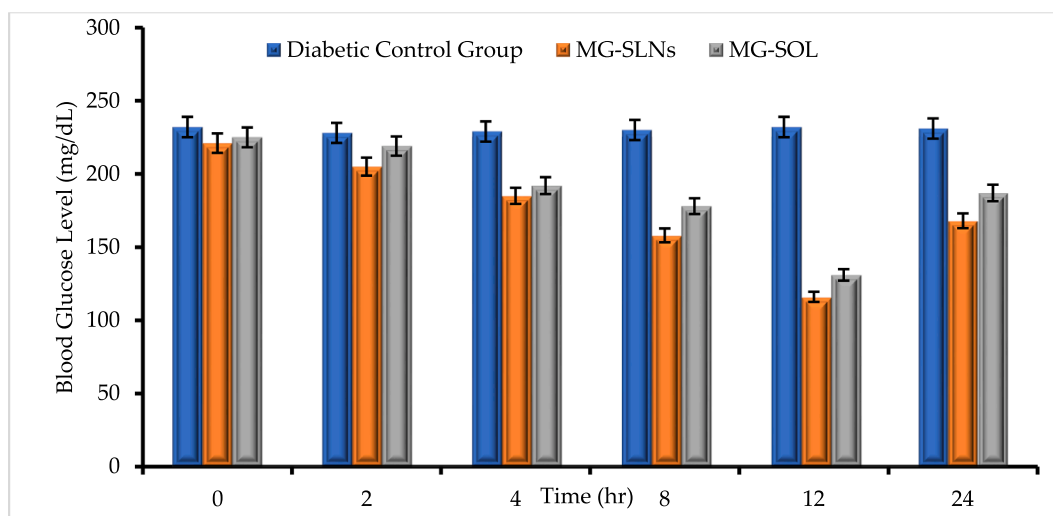


Fig. 14. Antidiabetic evaluation of MG-SLNs and MG-SOL against Diabetic control group.

**Table 3**  
Comparative biochemical estimation in different groups.

Group	TC (mg/dl)	TG (mg/dl)	HDL (mg/dl)	SGPT (U/dl)	SGOT (U/dl)
Normal control	61.4	45.9	55.1	33.7	37.3
Diabetic control	132.7	68.1	28.4	63.8	63.9
MG-SOL	98.5	56.7	38.9	41.2	51.4
MG-SLNs	75.2	51.4	46.6	37.5	43.7

the series of 181.42 to 38.97 nm. As per the DOE, Effect of variables on PS - the amount of both solid lipid and surfactant in combination indicated a negative impact. Similarly, surfactant concentration and sonication time in combination indicated a negative impact on the PS. Effect of variables on EE - the increment in the amount of the solid lipid resulted in an upsurge in the EE due to the entrapping of the drugs in large amounts. Also, the rise in the amount of the surfactant caused a rise in the EE of the MG due to the manifolds of the layers of surfactant

**Table 4**  
Independent and dependent variables used in CCRD.

Factors	Levels used				
	Axial	Low (-1)	Medium (0)	High (+1)	Axial
A-Solid lipid concentration (% w/v)	1.318	2	1	3	4.681
B-Surfactant concentration (% v/v)	2.318	3	4	5	5.681
C-Sonication time (sec)	65.910	100	150	200	234.09
<b>Dependent Factors</b>	<b>Constraints used</b>				
R1 - Particle size (nm)	Minimum				
R2 - Entrapment efficiency (%)	Maximum				

around the particle of the formation. Tween 80 has a high probable to increase the solubilization of the drug.

After applying CCRD, the optimized MG SLNs were prepared by taking 3 % w/v solid lipid mixture and 4 % v/v of the concentration of

surfactant, followed by sonication for 150 sec. The % cumulative quantity of MG released from MG-SLNs and MG-SOL in 0.1 N HCl was observed to be  $79.12 \pm 4.87\%$  and  $37.26 \pm 2.99\%$ , respectively. In PBS (pH 7.4), it was found to be  $80.21 \pm 5.61\%$  and  $36.07 \pm 3.04\%$ , respectively. According to the images, it can be well understood the formulation treated with dye was able to permeate deeper, i.e., 30  $\mu\text{m}$ , in comparison to the rhodamine hydro-ethanolic solution. The  $\text{IC}_{50}$  value of the AA, MG-SOL, and MG-SLNs were observed to be 23.33  $\mu\text{g/mL}$ , 49.08  $\mu\text{g/mL}$ , and 46.14  $\mu\text{g/mL}$ , accordingly. The findings of the docking study led us to conduct mangiferin formulations mediated *in-vitro*  $\alpha$ -amylase activity, the results of which have been presented in the next section. Parallel to this, different studies have shown the enzyme inhibitory nature of MG, in which MG significantly reduced the activity of the  $\alpha$ -amylase thus, acting against diabetes. Additionally, we compared the results to acarbose. Our findings indicate that MG-SLN exhibited a remarkable  $\alpha$ -glucosidase inhibition of  $68.76 \pm 3.14\%$ , whereas acarbose displayed an inhibition of  $63.43 \pm 4.02\%$ . These findings confirm that MG is more therapeutically effective when encapsulated in SLN formulation. These results suggest that both MG-SOL and MG-SLNs significantly improved the biochemical alterations associated with diabetes.

## 5. Conclusion

Utilizing CCRD, the MG-loaded SLN was successfully created and optimized. Additionally, this formulation has the desired properties that were necessary for oral MG administration to the target site. The refined formulation additionally demonstrated a discernible release in the MG from the SLN as opposed to the SOL. The permeation investigation also demonstrated the deeper MG penetration from the MG-SLNs. When the DPPH investigation was conducted, MG-SLN and MG-SOL significantly reduced the amount of oxygen species that would otherwise cause the level of glucose to rise, acting as effective anti-diabetic drugs. Lastly, the anti-diabetic profile of the developed formulation was further justified by performing a molecular docking study, *in-vitro*  $\alpha$ -amylase and  $\alpha$ -glucosidase inhibitory activity assay. The study demonstrated an enhancement in the inhibitory profile of MG-SLN in comparison MG-SOL. The developed MG-SLNs also showed promising antidiabetic properties. Therefore, the study could be concluded by justifying the fruitful optimization of MG-SLNs and their efficacy in increasing the orally bioavailability and therapeutic effectiveness of the MG. Moreover, this finding also indicates the transporting efficiency of SLNs in the targeted delivery of the drug (MG). Nevertheless, this study still lacks data from clinical studies, which would later help in achieving the therapeutic effectiveness of MG along with the risk and benefits in human.

## CRedit authorship contribution statement

**Ahmed I. Foudah:** Conceptualization, Funding acquisition, Writing – original draft, Writing – review & editing, Methodology, Supervision, Project administration, Software. **Mohammad Ayman Salkini:** Data curation, Investigation, Formal analysis, Methodology. **Mohammed H. Alqarni:** Funding acquisition, Writing – original draft, Validation, Resources. **Aftab Alam:** Conceptualization, Writing – original draft, Investigation, Supervision.

## Declaration of competing interest

The authors declare that they have no known competing financial interests or personal relationships that could have appeared to influence the work reported in this paper.

## Acknowledgement

The authors extend their appreciation to the Deputyship for Research

& Innovation, Ministry of Education in Saudi Arabia, for funding this research work through project number (IF2/PSAU/2022/03/22664).

**Institutional Review Board Statement:** The Standing Committee on Bioethics of Prince Sattam Bin Abdulaziz University's (PSAU) Animal-Care Guidelines (SCBR-20/2023), Al-Kharj, Ministry of Education, Kingdom of Saudi Arabia, have been approved to all experimental procedures and animal care.

## References

- Ahmad, N., Ahmad, R., Alam, A., Ahmad, F.J., 2018. Enhancement of oral bioavailability of doxorubicin through surface modified biodegradable polymeric nanoparticles. *Chem. Cent. J.* 12, 65. <https://doi.org/10.1186/s13065-018-0434-1>.
- Alam, T., Khan, S., Gaba, B., Haider, M.F., Baboota, S., Ali, J., 2018. Adaptation of Quality by Design-Based Development of Isradipine Nanostructured-Lipid Carrier and Its Evaluation for In Vitro Gut Permeation and In Vivo Solubilization Fate. *J. Pharm. Sci.* 107, 2914–2926. <https://doi.org/10.1016/j.xphs.2018.07.021>.
- Arrua, E.C., Hartwig, O., Ho, D.K., Loretz, B., Murgia, X., Salomon, C.J., Lehr, C.M., 2021. Surfactant-Free Glibenclamide Nanoparticles: Formulation, Characterization and Evaluation of Interactions with Biological Barriers. *Pharm. Res.* 38, 1081–1092. <https://doi.org/10.1007/S11095-021-03056-2>.
- Behbahani, E.S., Ghaedi, M., Abbaspour, M., Rostamizadeh, K., 2017. Optimization and characterization of ultrasound assisted preparation of curcumin-loaded solid lipid nanoparticles: Application of central composite design, thermal analysis and X-ray diffraction techniques. *Ultrason. Sonochem.* 38, 271–280. <https://doi.org/10.1016/j.ultrsonch.2017.03.013>.
- Capetti, F., Cagliero, C., Marengo, A., Bicchi, C., Rubiolo, P., Sgorbini, B., 2020. Bio-guided fractionation driven by *in vitro*  $\alpha$ -amylase inhibition assays of essential oils bearing specialized metabolites with potential hypoglycemic activity. *Plants* 9, 1–17. <https://doi.org/10.3390/plants9091242>.
- Chaudhury, A., Duvoor, C., Dendi, V.S.R., Kraleti, S., Chada, A., Ravilla, R., Marco, A., Shekhawat, N.S., Montales, M.T., Kuriakose, K., Sasapu, A., Beebe, A., Patil, N., Musham, C.K., Lohani, G.P., Mirza, W., 2017. Clinical Review of Antidiabetic Drugs: Implications for Type 2 Diabetes Mellitus Management. *Front. Endocrinol. Lausanne*, 8, 6. <https://doi.org/10.3389/FENDO.2017.00006>.
- Cirri, M., Maestrelli, F., Mura, P., Ghelardini, C., Di, L., Mannelli, C., 2018. Combined approach of cyclodextrin complexation and nanostructured lipid carriers for the development of a pediatric liquid oral dosage form of hydrochlorothiazide. *Pharmaceutics* 10, 287. <https://doi.org/10.3390/pharmaceutics10040287>.
- Cometa, S., Bonifacio, M.A., Trapani, G., Di Gioia, S., Dazzi, L., De Giglio, E., Trapani, A., 2020. In vitro investigations on dopamine loaded Solid Lipid Nanoparticles. *J. Pharm. Biomed. Anal.* 185, 113257. <https://doi.org/10.1016/j.jpba.2020.113257>.
- Danaei, M., Dehghankhold, M., Ataei, S., Davarani, F.H., Javanmard, R., Dokhani, A., Khorasani, S., Mozafari, M.R., 2018. Impact of particle size and polydispersity index on the clinical applications of lipidic nanocarrier systems. *Pharmaceutics* 10, 57. <https://doi.org/10.3390/pharmaceutics10020057>.
- Dar, A., Faizi, S., Naqvi, S., Roome, T., Zikr-Ur-Rehman, S., Ali, M., Firdous, S., Moin, S.T., 2005. Analgesic and Antioxidant Activity of Mangiferin and Its Derivatives: the Structure Activity Relationship. *Biol. Pharm. Bull.* 28, 596–600. <https://doi.org/10.1248/BPB.28.596>.
- Date, K., Yamazaki, T., Toyoda, Y., Hoshi, K., Ogawa, H., 2020.  $\alpha$ -Amylase expressed in human small intestinal epithelial cells is essential for cell proliferation and differentiation. *J. Cell. Biochem.* 121, 1238–1249. <https://doi.org/10.1002/JCB.29357>.
- Donga, S., Chanda, S., 2021. Facile green synthesis of silver nanoparticles using *Mangifera indica* seed aqueous extract and its antimicrobial, antioxidant and cytotoxic potential (3-in-1 system). *Artif. Cells, Nanomedicine, Biotechnol.* 49, 292–302. <https://doi.org/10.1080/21691401.2021.1899193>.
- Duong, V., Nguyen, T., Molecules, H.M., 2020. U., 2020. Preparation of solid lipid nanoparticles and nanostructured lipid carriers for drug delivery and the effects of preparation parameters of solvent injection method. *Molecules* 25, 4781. <https://doi.org/10.3390/molecules25204781>.
- Friesner, R.A., Banks, J.L., Murphy, R.B., Halgren, T.A., Klicic, J.J., Mainz, D.T., Repasky, M.P., Knoll, E.H., Shelley, M., Perry, J.K., Shaw, D.E., Francis, P., Shenkin, P.S., 2004. Glide: A New Approach for Rapid, Accurate Docking and Scoring. 1. Method and Assessment of Docking Accuracy. *J. Med. Chem.* 47, 1739–1749. [https://doi.org/10.1021/JM0306430/SUPPL\\_FILE/JM0306430\\_S.PDF](https://doi.org/10.1021/JM0306430/SUPPL_FILE/JM0306430_S.PDF).
- Friesner, R.A., Murphy, R.B., Repasky, M.P., Frye, L.L., Greenwood, J.R., Halgren, T.A., Sanschagrin, P.C., Mainz, D.T., 2006. Extra precision glide: Docking and scoring incorporating a model of hydrophobic enclosure for protein-ligand complexes. *J. Med. Chem.* 49, 6177–6196. [https://doi.org/10.1021/JM051256O/SUPPL\\_FILE/JM051256OSI20060602\\_023733.PDF](https://doi.org/10.1021/JM051256O/SUPPL_FILE/JM051256OSI20060602_023733.PDF).
- Gaba, B., Fazil, M., Khan, S., Ali, A., Baboota, S., Ali, J., 2015. Nanostructured lipid carrier system for topical delivery of terbinafine hydrochloride. *Bull. Fac. Pharmacy, Cairo Univ.* 53, 147–1119. <https://doi.org/10.1016/j.bfopcu.2015.10.001>.
- Gaurav, Z.S., Parveen, B., Ibrahim, M., Sharma, I., Sharma, S., Sharma, A.K., Parveen, R., Ahmad, S., 2020. TLC-MS bioautography-based identification of free-radical scavenging,  $\alpha$ -amylase, and  $\alpha$ -glucosidase inhibitor compounds of antidiabetic tablet BGR-34. *ACS Omega* 5, 29688–29697. <https://doi.org/10.1021/ACSEOMEGA.0C02995>.
- Hassan, H., Adam, S.K., Alias, E., Affandi, M.M.R.M.M., Shamsuddin, A.F., Basir, R., 2021. Central Composite Design for Formulation and Optimization of Solid Lipid

- Nanoparticles to Enhance Oral Bioavailability of Acyclovir. *Molecules* 26, 5432. <https://doi.org/10.3390/MOLECULES26185432>.
- Ichiki, H., Miura, T., Kubo, M., Ishihara, E., Komatsu, Y., Tanigawa, K., Okada, M., 1998. New Antidiabetic Compounds, Mangiferin and Its Glucoside. *Biol. Pharm. Bull.* 21, 1389–1390. <https://doi.org/10.1248/BBP.21.1389>.
- Imran, M., Iqbal, M.K., Imtiyaz, K., Saleem, S., Mittal, S., Rizvi, M.M.A., Ali, J., Baboota, S., 2020. Topical nanostructured lipid carrier gel of quercetin and resveratrol: Formulation, optimization, in vitro and ex vivo study for the treatment of skin cancer. *Int. J. Pharm.* 587, 119705 <https://doi.org/10.1016/j.ijpharm.2020.119705>.
- Iqbal, M.K., Iqbal, A., Imtiyaz, K., Rizvi, M.M.A., Gupta, M.M., Ali, J., Baboota, S., 2021. Combinatorial lipid-nanosystem for dermal delivery of 5-fluorouracil and resveratrol against skin cancer: Delineation of improved dermatokinetics and epidermal drug deposition enhancement analysis. *Eur. J. Pharm. Biopharm.* 163, 223–239. <https://doi.org/10.1016/j.ejpb.2021.04.007>.
- Jazuli, I., Annu, N.B., Moolakkadath, T., Alam, T., Baboota, S., Ali, J., 2019. Optimization of Nanostructured Lipid Carriers of Lurasidone Hydrochloride Using Box-Behnken Design for Brain Targeting. In *Vitro and In Vivo Studies*. *J. Pharm. Sci.* 108, 3082–3090. <https://doi.org/10.1016/j.xphs.2019.05.001>.
- Keum, C.G., Noh, Y.W., Baek, J.S., Lim, J.H., Hwang, C.J., Na, Y.G., Shin, S.C., Cho, C.W., 2011. Practical preparation procedures for docetaxel-loaded nanoparticles using polylactic acid-co-glycolic acid. *Int. J. Nanomedicine* 6, 2225–2234. <https://doi.org/10.2147/IJN.S24547>.
- Khan, S., Shaharyar, M., Fazil, M., Baboota, S., Ali, J., 2016. Tacrolimus-loaded nanostructured lipid carriers for oral delivery – Optimization of production and characterization. *Eur. J. Pharm. Biopharm.* 108, 277–288. <https://doi.org/10.1016/j.ejpb.2016.07.017>.
- Kharroubi, A.T., 2015. Diabetes mellitus: The epidemic of the century. *World J. Diabetes* 6, 850. <https://doi.org/10.4239/WJD.V6.I6.850>.
- Kothari, A., Rajagopalan, P., 2020. The assembly of integrated rat intestinal-hepatocyte cultures. *Bioeng. Transl. Med.* 5, e10146.
- Leaves, L., *Ethnomedicine*, L.L.-A.J. of, 2014, U., 2014. Antioxidant activity by DPPH radical scavenging method of *ageratum conyzoides*. *Am. J. Ethnomedicine* 1, 244–249.
- Li, H.L., Zhao, X.B., Ma, Y.K., Zhai, G.X., Li, L.B., Lou, H.X., 2009. Enhancement of gastrointestinal absorption of quercetin by solid lipid nanoparticles. *J. Control. Release* 133, 238–244. <https://doi.org/10.1016/j.jconrel.2008.10.002>.
- Liu, M., Liu, Y., Ge, Y., Zhong, Z., Wang, Z., Wu, T., Zhao, X., Zu, Y., 2020. Solubility, antioxidant, and oral bioavailability improvement of mangiferin microparticles prepared using the supercritical antisolvent method. *Pharmaceutics* 12, 90. <https://doi.org/10.3390/pharmaceutics12020090>.
- Loo, C.H., Basri, M., Ismail, R., Lau, H.L.N., Tejo, B.A., Kanthimathi, M.S., Hassan, H.A., Choo, Y.M., 2013. Effect of compositions in nanostructured lipid carriers (NLC) on skin hydration and occlusion. *Int. J. Nanomedicine* 8, 13–22. <https://doi.org/10.2147/IJN.S35648>.
- Madan, J., Dua, K., Khude, P., 2014. Development and evaluation of solid lipid nanoparticles of mometasone furoate for topical delivery. *Int. J. Pharm. Investig.* 4, 60. <https://doi.org/10.4103/2230-973X.133047>.
- Mahajan, H., Patil, N., 2021. Nanoemulsion containing a synergistic combination of curcumin and quercetin for nose-To-brain delivery: In vitro and in vivo studies. *Asian Pac. J. Trop. Biomed.* 11, 510–518. <https://doi.org/10.4103/2221-1691.328058>.
- Mahapatra, M.K., Kumar, R., Malla, P., Kumar, M., 2014. In silico accounting of novel pyridazine analogues as h-PTP 1B inhibitors: Pharmacophore modelling, atom-based 3D QSAR and docking studies. *Med. Chem. Res.* 23, 2701–2711. <https://doi.org/10.1007/S00044-013-0797-8>.
- Mersad Sefidgar, S., Ahmadi-Hamedani, M., Javan, A.J., Sani, R.N., Vayghan, A.J., n.d. Effect of crocin on biochemical parameters, oxidative/antioxidative profiles, sperm characteristics and testicular histopathology in streptozotocin-induced diabetic rats. *Orig. Res. Artic.* 9, 347–361.
- Miura, T., Ichiki, H., Hashimoto, I., Iwamoto, N., Kao, M., Kubo, M., Ishihara, E., Komatsu, Y., Okada, M., Ishida, T., Tanigawa, K., 2001. Antidiabetic activity of a xanthone compound, mangiferin. *Phytomedicine* 8, 85–87. <https://doi.org/10.1078/0944-7113-00009>.
- Mukherjee, S., Ray, S., Thakur, R.S., 2009. Solid lipid nanoparticles: A modern formulation approach in drug delivery system. *Indian J. Pharm. Sci.* 71, 349–358. <https://doi.org/10.4103/0250-474X.57282>.
- Nabi, S.A., Kasetti, R.B., Sirasanagandla, S., Tilak, T.K., Venkateshwarulu, M., Kumar, J., Rao, C.A., 2013. Antidiabetic and antihyperlipidemic activity of Piper longum root aqueous extract in STZ induced diabetic rats. *BMC Complement. Altern. Med.* 13, 1–9. <https://doi.org/10.1186/1472-6882-13-37>.
- Naseri, N., Valizadeh, H., Zakeri-Milani, P., 2015. Solid Lipid Nanoparticles and Nanostructured Lipid Carriers: Structure. Preparation and Application. *Adv. Pharm. Bull.* 5, 305. <https://doi.org/10.15171/APB.2015.043>.
- Ngo, D.-H., Ngo, D.-N., Thanh, T., Vo, N., Vo, T.S., 2019. Scientia Pharmaceutica Mechanism of Action of Mangifera indica Leaves for Anti-Diabetic Activity. *Sci. Pharm.* 87, 13. <https://doi.org/10.3390/scipharm87020013>.
- Pandey, S., Patel, P., Gupta, A., 2018. Novel Solid Lipid Nanocarrier of Glibenclamide: A Factorial Design Approach with Response Surface Methodology. *Curr. Pharm. Des.* 24, 1811–1820. <https://doi.org/10.2174/1381612824666180522092743>.
- Philip, D., 2011. Mangifera Indica leaf-assisted biosynthesis of well-dispersed silver nanoparticles. *Spectrochim. Acta - Part A Mol. Biomol. Spectrosc.* 78, 327–331. <https://doi.org/10.1016/j.saa.2010.10.015>.
- Picot, M.C.N., Zengin, G., Mollica, A., Stefanucci, A., Carradori, S., Mahomoodally, M.F., 2017. In vitro and in silico Studies of Mangiferin from *Aphloia theiformis* on Key Enzymes Linked to Diabetes Type 2 and Associated Complications. *Med. Chem. (Los Angeles)*. 13, 633–640. <https://doi.org/10.2174/1573406413666170307163929>.
- Qamar, Z., Ashhar, M.U., Annu, Q.F.F., Sahoo, P.K., Ali, A., Ali, J., Baboota, S., 2021. Lipid nanocarrier of selegiline augmented anti-Parkinson's effect via P-gp modulation using quercetin. *Int. J. Pharm.* 609, 121131 <https://doi.org/10.1016/j.ijpharm.2021.121131>.
- Samadarsi, R., Dutta, D., 2019. Design and characterization of mangiferin nanoparticles for oral delivery. *J. Food Eng.* 247, 80–94. <https://doi.org/10.1016/j.jfoodeng.2018.11.020>.
- Samanta, S., 2022. Anti-diabetic activity of mango (*Mangifera indica*): a review. *MOJ Bioequiv Availab* 6, 23–26. <https://doi.org/10.15406/mojbb.2019.06.00131>.
- Santonocito, D., Viviero-Lopez, M., Lauro, M.R., Torrisi, C., Castelli, F., Sarpietro, M.G., Puglia, C., 2022. Design of Nanotechnological Carriers for Ocular Delivery of Mangiferin: Preformulation Study. *Molecules* 27, 1328. <https://doi.org/10.3390/MOLECULES27041328>.
- Sapra, A., Bhandari, P., 2021. *Diabetes Mellitus*. StatPearls Publishing, Treasure Island (FL) <https://pubmed.ncbi.nlm.nih.gov/31855345/> (accessed 10.28.23).
- Schrödinger., 2021. [WWW Document], n.d. URL <https://www.schrodinger.com/releases/release-2021-2> (accessed 10.28.23).
- Sekar, V., Chakraborty, S., Mami, S., Sali, V.K., Vasanthi, H.R., 2019. Mangiferin from *Mangifera indica* fruits reduces post-prandial glucose level by inhibiting  $\alpha$ -glucosidase and  $\alpha$ -amylase activity. *South African J. Bot.* 120, 129–134. <https://doi.org/10.1016/J.SAJB.2018.02.001>.
- Sun, H., Saeedi, P., Karuranga, S., Pinkepank, M., Ogurtsova, K., Duncan, B.B., Stein, C., Basit, A., Chan, J.C.N., Mbanya, J.C., Pavkov, M.E., Ramachandran, A., Wild, S.H., James, S., Herman, W.H., Zhang, P., Bommer, C., Kuo, S., Boyko, E.J., Magliano, D. J., 2022. IDF Diabetes Atlas: Global, regional and country-level diabetes prevalence estimates for 2021 and projections for 2045. *Diabetes Res. Clin. Pract.* 183, 109119 <https://doi.org/10.1016/j.diabres.2021.109119>.
- Tahir, H.U., Sarfraz, R.A., Ashraf, A., Adil, S., 2016. Chemical Composition and Antidiabetic Activity of Essential Oils Obtained from Two Spices (*Syzygium aromaticum* and *Cuminum cyminum*). *Int. J. Food Prop.* 19, 2156–2164. <https://doi.org/10.1080/10942912.2015.1110166>.
- Thaipong, K., Boonprakob, U., Crosby, K., Cisneros-Zevallos, L., Hawkins Byrne, D., 2006. Comparison of ABTS, DPPH, FRAP, and ORAC assays for estimating antioxidant activity from guava fruit extracts. *J. Food Compos. Anal.* 19, 669–675. <https://doi.org/10.1016/j.jfca.2006.01.003>.
- Trinder, P., 1969. Determination of Glucose in Blood Using Glucose Oxidase with an Alternative Oxygen Acceptor. *Ann. Clin. Biochem.* 6, 24–27. <https://doi.org/10.1177/000456326900600108>.
- Üner, M., Yener, G., 2007. Importance of solid lipid nanoparticles (SLN) in various administration routes and future perspectives. *Int. J. Nanomedicine* 2, 289–300. <https://doi.org/10.2147/IJN.S2.3.289>.
- Varshosaz, J., Ghaffari, S., Khoshayand, M.R., Atyabi, F., Azarmi, S., Kobarfard, F., 2010. Development and optimization of solid lipid nanoparticles of amikacin by central composite design. *J. Liposome Res.* 20, 97–104. <https://doi.org/10.3109/08982100903103904>.
- Weng, J., Tong, H.H., Chow, S.F., 2020 Aug 4. In vitro release study of the polymeric drug nanoparticles: development and validation of a novel method. *Pharmaceutics* 12 (8), 732. <https://doi.org/10.3390/pharmaceutics12080732>.
- Wu, L., Zhao, L., Su, X., Zhang, P., Ling, G., 2020. Repaglinide-loaded nanostructured lipid carriers with different particle sizes for improving oral absorption: preparation, characterization, pharmacokinetics, and in situ intestinal perfusion. *Drug Deliv.* 27, 400–409. <https://doi.org/10.1080/10717544.2019.1689313>.
- Zhang, Z., Lu, Y., Qi, J., Wu, W., 2021. An update on oral drug delivery via intestinal lymphatic transport. *Acta Pharm. Sin. B* 11, 2449–2468. <https://doi.org/10.1016/J.APSB.2020.12.022>.